Climate Dynamics
https://doi.org/10.1007/s00382-020-05180-y

South Asian monsoon response to weakening of Atlantic meridional overturning circulation in a warming climate

N. Sandeep[1,2] · P. Swapna[1] · R. Krishnan[1] · R. Farneti[3] · A. G. Prajeesh[1] · D. C. Ayantika[1] · S. Manmeet[1]

Received: 10 June 2019 / Accepted: 20 February 2020

Abstract
Observational records and climate model projections reveal a considerable decline in the Atlantic Meridional Overturning Circulation (AMOC). Changes in the AMOC can have a significant impact on the global climate. Sustained warming due to increased greenhouse gas emissions is projected to weaken the AMOC, which in turn can lead to changes in the location of Inter-tropical convergence zone (ITCZ), oceanic and atmospheric large-scale circulation, tropical precipitation and regional monsoons. Using proxy records, observations and CMIP6 simulations of IITM Earth System Model (IITM-ESM), we investigate the changes in the AMOC and associated changes in the large-scale circulation and precipitation patterns over the South Asian monsoon region. Transient CO_2 simulation and additional model sensitivity experiments with realistic surface heat and freshwater perturbation anomalies under the experimental protocol of Flux Anomaly Forcing Model Intercomparison Project (FAFMIP) performed with IITM-ESM reveal a decline in the strength of AMOC. The weakening of AMOC is associated with enhanced heat and freshwater forcing in the North Atlantic resulting in the reduction of northward oceanic heat transport and an enhanced northward atmospheric heat transport. Changes in AMOC lead to weakening of large-scale north–south temperature gradient and regional land-sea thermal gradient, which in turn weaken the regional Hadley circulation and, monsoon circulation over the South Asian region. Both the FAFMIP and transient CO_2 experiments reveal consistent results of weakening South Asian Monsoon circulation with a decline of AMOC, while precipitation exhibits contrasting responses as precipitation changes are dominated by the thermodynamic response. The suite of observational and numerical analysis provides a mechanistic hypothesis for the weakening of South Asian monsoon circulation concomitant with a weakening of AMOC in a warming climate.

Keywords Atlantic meridional overturning circulation · South Asian monsoon · Weakening of circulation · Heat transport · Global warming

1 Introduction

The Atlantic Meridional Overturning Circulation (AMOC) is an important component of Earth's climate system. The AMOC transports a large fraction of ocean heat and carbon and is associated with the production of about half of the global ocean's deep waters in the northern Atlantic (Srokosz et al. 2012; Rhein 2014; Buckley and Marshall 2016; Trenberth and Fasullo 2017). The AMOC heat transport accounts for 25% of maximum global ocean meridional heat transport required by the coupled ocean–atmosphere system to maintain the radiation budget (Trenberth and Fasullo 2017). The Intergovernmental Panel on Climate Change (IPCC) AR5 considers it very likely that the AMOC will weaken in the 21st century as a consequence of anthropogenic greenhouse gas emissions (Stocker et al. 2013). The weakening of AMOC can lead to a significant reduction of oceanic heat supply to the North Atlantic region. The CMIP5 models projected a reduction of AMOC on the order of 11% in RCP2.6 scenario and 34% for the RCP8.5 scenario.

Changes in the strength of AMOC can impact the global climate. Previous studies have documented that the changes in strength of AMOC can impact North Atlantic storm tracks

✉ N. Sandeep
sandeep.cat@tropmet.res.in

1 Centre for Climate Change Research, Indian Institute of Tropical Meteorology, Pune 411008, India

2 Department of Atmospheric and Space Sciences, Savitribai Phule Pune University, Pune, India

3 Earth System Physics Section, International Centre for Theoretical Physics, Trieste, Italy

Published online: 27 February 2020

(Woollings et al. 2012), the inter tropical convergence zone (ITCZ; Vellinga and Wood 2002; Chiang et al. 2008; Cheng et al. 2013), North American and European summer climate (Sutton and Hodson 2005; Parsons et al. 2014), African and South Asian monsoon rainfall (Zhang and Delworth 2006; Mohtadi et al. 2014). The variability in AMOC has been linked to the variability of south Asian monsoon through changes in the ITCZ. Zhang and Delworth (2005), using idealized experiments, have shown that excessive freshening in the north Atlantic can lead to a weakening of AMOC and a weakening of South Asian monsoon. All of the above studies documented the association between weakening AMOC and South Asian summer monsoon rainfall using various coupled models. Most of the studies including Zhang and Delworth (2005) addressed the impact of freshening on the AMOC weakening and its association to South Asian summer monsoon. However, Gregory et al. (2016a, b) have shown that the response of AMOC to heat flux perturbation is larger than due to the fresh water flux perturbation. This has been supported by the previous studies (Delworth et al. 1993; Griffies and Tziperman 1995; Delworth and Greatbatch 2000). But, none of the previous studies addressed the impact of increased heating on weakening the AMOC and its impact on South Asian summer monsoon. The novelty of the study is that we propose a mechanism for the association of AMOC to South Asian Monsoon under a warming climate and show that South Asian monsoon circulation weakens in response to weakening AMOC, while precipitation changes are dominated by thermodynamics response. Also, we decompose the water vapor budget into dynamic and thermodynamic components and provide explanation on the response of precipitation and circulation to projected changes of AMOC in a warming climate.

An increase in atmospheric greenhouse gases (GHG) is expected to affect the large-scale circulation and precipitation patterns. An increase in atmospheric moisture due to atmospheric warming, acts to enhance precipitation, while circulation is projected to weaken with increased stability of the atmosphere (Endo and Kitoh 2014; Li et al. 2015; Mei et al. 2015). Enhanced warming due to an increase in GHG is projected to weaken the AMOC (Jackson 2013), which in turn can affect the large-scale circulation and precipitation patterns (Vellinga and Wood 2008; Liu and Fedorov 2019). Energetics arguments suggest that AMOC weakening can cause a southward shift of ITCZ and affect regional monsoons (Donohoe et al. 2013). Understanding the circulation and precipitation changes to a substantial decline in AMOC as projected by the IPCC models is vital given that nearly half of the world's population in the South Asian region heavily relies on monsoon for agriculture, food, and energy security.

Observational records also indicate a twentieth-century slowdown in AMOC. The annual mean temperature trends from 1901 to 2013 show patterns of cooling in the North Atlantic associated with weakening of AMOC (Rahmstorf et al. 2015). The AMOC index (based on Rahmstorf et al. 2015) shows that there is a large decline in the strength of AMOC after 1975 (Dickson et al. 1988; Belkin et al. 1998). The daily mean AMOC transport from RAPID-MOCHA array along 26.5 N available from 2004 shows that AMOC is not stable and has high temporal variability (Cunningham et al. 2007; Kanzow et al. 2007, 2010a; Johns et al. 2008, 2011; Rayner et al. 2011).

In the background of global warming and projected weakening of AMOC, we explore the links between the unprecedented decline in the strength of AMOC and its impact on the circulation and precipitation patterns over the South Asian region using IITM-ESM CMIP6 simulations. We further perform a set of idealized experiments with extreme warming, extreme freshening scenarios under the protocol of Flux Anomaly Forcing Model Intercomparison (FAFMIP) (Gregory et al. 2016a) and transient CO_2 simulations to better understand the association between weakening of AMOC and South Asian monsoon circulation and precipitation. Section 2 describes the model, experiment design, data and methodology. Section 3 consists of the validation of the model (IITM-ESM) used for the analysis. The dynamic and thermodynamic responses of monsoon precipitation and circulation to changes to the decline of AMOC and a mechanistic hypothesis for the future changes in the South Asian monsoon circulation in response to the weakening of AMOC in a warming climate are discussed in subsequent sections. The summary and conclusion from the study are discussed in the last section.

2 Model description, experiments, and data sets

2.1 Model

The model used for the study is a global coupled ocean–atmosphere general circulation model, the IITM-Earth System Model (IITM-ESM, Swapna et al. 2018a), developed at the Indian Institute of Tropical Meteorology (IITM). IITM-ESM comprises of Global Forecast System (GFS; Moorthi et al. 2001) as the atmospheric component based on the National Centre for Environmental Prediction (NCEP, Saha et al. 2014). GFS is a spectral model with a triangular truncation of 62 waves (T62). The horizontal resolution is approximately 2^0 (~ 200 km) and vertical resolution comprises 64 sigma-pressure hybrid layers with top model layer extending up to 0.2 hPa. The land model is NOAH-LSM consisting of four soil layers, 13 vegetation types and nine soil types. More description of NOAH-LSM can be obtained from Ek (2003).

The ocean model in IITM-ESM is the NOAA/GFDL Modular Ocean Model Version 4p1 (MOM4p1, Griffies 2009). MOM4p1 is a hydrostatic model configured using the Boussinesq approximation and a rescaled geopotential vertical coordinate. The zonal resolution is 1° and the meridional resolution is 0.33° between 10 S and 10 N and gradually increasing to 1° poleward of 30°S and 30° N with 50 vertical levels. The Sea ice model in IITM-ESM is the Sea Ice Simulator (SIS, Winton 2000). SIS is a dynamical model with three vertical layers, one snow, and two ice layers. The Sea ice is classified into five ice thickness categories (Delworth et al. 2006).

2.2 Experimental set-up

To understand the responses of the large-scale circulation and precipitation to the weakening of the AMOC, we utilize IITM-ESM CMIP6 simulations and sensitivity experiments which are described in detail in Table 1. The model reproduces realistic pre-industrial climate using 1850 trace gas concentrations, solar irradiance, anthropogenic aerosols, and land-use land-cover conditions under the CMIP6 protocol for the pre-industrial control (piControl) simulation as discussed in Swapna et al. (2018b).

A FAF-HEAT simulation experiment is conducted with the net surface heat flux anomaly forcing provided by FAFMIP starting from the piControl state as suggested by Gregory et al. (2016b). The model-mean surface heat flux anomaly from 13 CMIP5 models was used as the surface flux anomaly forcing. The heat flux anomaly imposed is computed as the difference in net surface heat flux between the climatological monthly time means of years 61–80 of 1 pct CO_2 and the corresponding 20 years of piControl. The imposed heat flux anomaly is added only to the momentum balance of the ocean water surface, but not the turbulent mixing scheme. This FAF-HEAT simulation is performed for 70 years and the last 10 years of data are used for the analysis. In the FAF-HEAT experiment, the strength of AMOC reduces from 15 Sv in the piControl (1 Sv = 10^6 m^3 s^{-1}) to 5 Sv.

A FAF-WATER simulation experiment is conducted with the surface freshwater flux anomaly (i.e. precipitation–evaporation) forcing provided by FAFMIP starting from the piControl state (Gregory et al. 2016a, b). Similar to the FAF-HEAT, the fresh water flux anomaly is added to the ocean surface. This FAF-WATER simulation is also performed for 70 years and the last 10 years of data are used for the analysis. In the FAF-WATER experiment, the AMOC strength reduces from 15 Sv in the piControl to 10 Sv. Similar sensitivities were also reported in Gregory et al. (2016a, b).

Additionally, a transient CO_2 increase experiment is performed with CO_2 concentration increasing at 1% per year starting from 1850 values until doubling and then held fixed for 100 more years, following the CMIP6 protocols. The AMOC, circulation, and precipitation changes during the last 50 years of the simulation are presented in the study.

2.3 Data sets used

The data sets used for evaluating model simulations are summarized here. The gridded monthly rainfall data from the Tropical Rainfall Measuring Mission (TRMM) Microwave Imager (TMI Huffman et al. 2007) for the period 1998–2012 is utilized. We use the temperature and salinity data from the World Ocean Atlas (WOA2009, Locarnini 2010), the Hadley Centre Sea Ice, and Sea Surface Temperature and sea-ice concentration data set (HadISST1.1, Rayner et al. 2003), Extended Reconstructed Sea Surface Temperature (ERSSTv4) for the period 1950–2012. RAPID MOCHA trans-basin array data from 2004 was used to understand the variations of AMOC strength. Vertical velocity data from Global Ocean Data Analysis system (GODAS) is used for the period 1980–2017.

3 Results

3.1 Association between AMOC and South Asian monsoon from long-term proxy records

The Asian summer monsoon records derived from Hulu cave in eastern China shows, during cold stadial condition in Greenland, the Asian summer monsoon was reduced (Wang

Table 1 List of experiments performed with the forcing used and the length of the simulation

Experiment	Forcing used	Length of the simulation
PI-Control	Preindustrial CMIP6 Forcing; GHG's, LULC and aerosols set to 1850 values.	300 year run (after 500 year of spin up)
FAF-HEAT	Net Surface heat flux anomaly (W m^{-2}) provided by FAFMIP project (Gregory et al. 2016a, 2016b)	70 years
FAF-WATER	Net Surface fresh water flux anomaly (kg m^{-2} s^{-1}) provided by FAFMIP project (Gregory et al. 2016a, 2016b)	70 years
1 pct CO2	CO2 concentration is increased at a rate of 1% per year up to 70 years and then kept constant	100 years

et al. 2001), and Indian summer monsoon was also shown to be weakened (Altabet et al. 2002) during the same period. These stadials have been associated with shift in the ITCZ and changes in South Asian monsoon strength (McGee et al. 2014).

Proxy record taken from Cariaco basin off the Venezuela coast during the past 14,000 years reveal the location of ITCZ (Haug et al. 2001). The location of ITCZ was estimated based on Titanium and Iron concentration data. This basin record shows robust correlations with climate records from distant regions and serves as evidence for the global teleconnections (Haug and Hughen 2000). Proxy records of Atlantic multidecadal variability (AMV) from AD 800–2010 taken from a network of terrestrial records from the North Atlantic region (Wang et al. 2017) serve as evidence for the changes in the AMOC strength (McCarthy et al. 2012). The association between the location of ITCZ and the strength of AMOC can be clearly noted from the long term records from the Cariaco basin and the terrestrial proxy record (Fig. 1). Time-series reveal a northward displacement of ITCZ during strong AMOC periods and vice versa.

Long term variations in precipitation were inferred based on amplitudes of the Iron (Fe) and Titanium (Ti) signals from ODP Site 1002 (10°42.739 N, 65°10.189 W) drilled at a water depth of 893 m where there exist anoxic conditions in the Cariaco water column. Higher precipitation rates are seen from AD 800–1300, the interval of time referred to as the "Medieval Warm Period." This was followed by the "Little Ice Age," marked by lower precipitation rates in the Cariaco region.

The association between ITCZ, AMOC and Indian summer monsoon rainfall can be seen from long-term Stalgamite records from Sahiya Cave of Northern India (30°36′N, 77°52′E) (Sinha et al. 2015). Analysis of the 1200 year long term proxy records (from AD 800–2000) of AMOC and Indian summer monsoon rainfall (ISMR) show a positive correlation ($r^2 = 0.45$) which is statistically significant at 99.9% confidence level (Fig. 1a). The significant correlation ascertains the relation between AMOC and ISMR. Similarly, the long term proxy records of ITCZ from the Caraiaco basin and AMOC also show a positive correlation ($r^2 = 0.48$) indicating a close relationship between the position of ITCZ and strength of AMOC (Fig. 1b). During periods of strong AMOC, ITCZ was shifted northward and ISMR showed enhanced precipitation over the Indian region (Fig. 1).

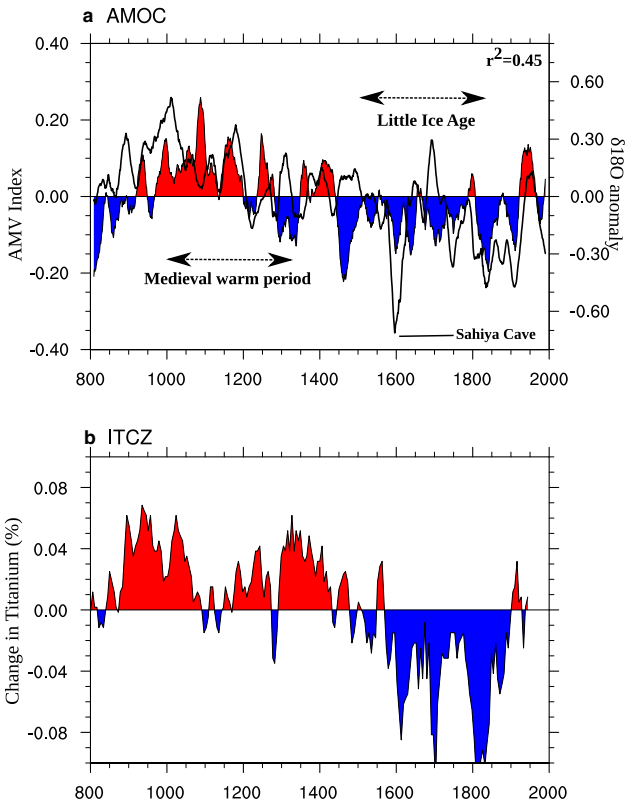

Fig. 1 **a** Time-series of AMV index (shaded) and Time-series of Sahiya cave rainfall data is shown as a black line **b** Time-series of the location of ITCZ from cariaco basin

4 Simulation of AMOC and South Asian monsoon in IITM-ESM

Before analyzing the links between AMOC and South Asian monsoon, we summarize the main characteristics of AMOC and South Asian monsoon in IITM-ESM.

4.1 AMOC characteristics in IITM-ESM

The piControl simulation of IITM-ESM was performed by prescribing the GHG, aerosol concentrations and land use land cover change to 1850 values according to CMIP6 protocol. The model is run for 500 years of spin-up to reach a stable quasi-equilibrium state which is a representation of the 1850 preindustrial climate. Since the representation of meridional ocean and atmospheric transport is crucial for a model, we first analyze AMOC, a major contributor of heat transport. The time series of annual mean AMOC for the last 300 year-long piControl simulation is shown in Fig. 2d. The simulated AMOC features are comparable with the corresponding piControl simulation of the CMIP5 multi-model mean (10 CMIP5 models are considered) and also with Global Ocean Data Assimilation (GODAS) as shown in Fig. 2. AMOC comprised of northward flow in the upper levels and southward return flow below 1000 m (Fig. 2a). The northward volume transport in IITM-ESM is around 15 Sv between 20^0 and 50^0 N (Fig. 2a) which is comparable to observational estimates of direct ocean measurements near 26.5^0 N from the RAPID array. The mean AMOC strength from the 300-year preindustrial simulation of IITM-ESM is

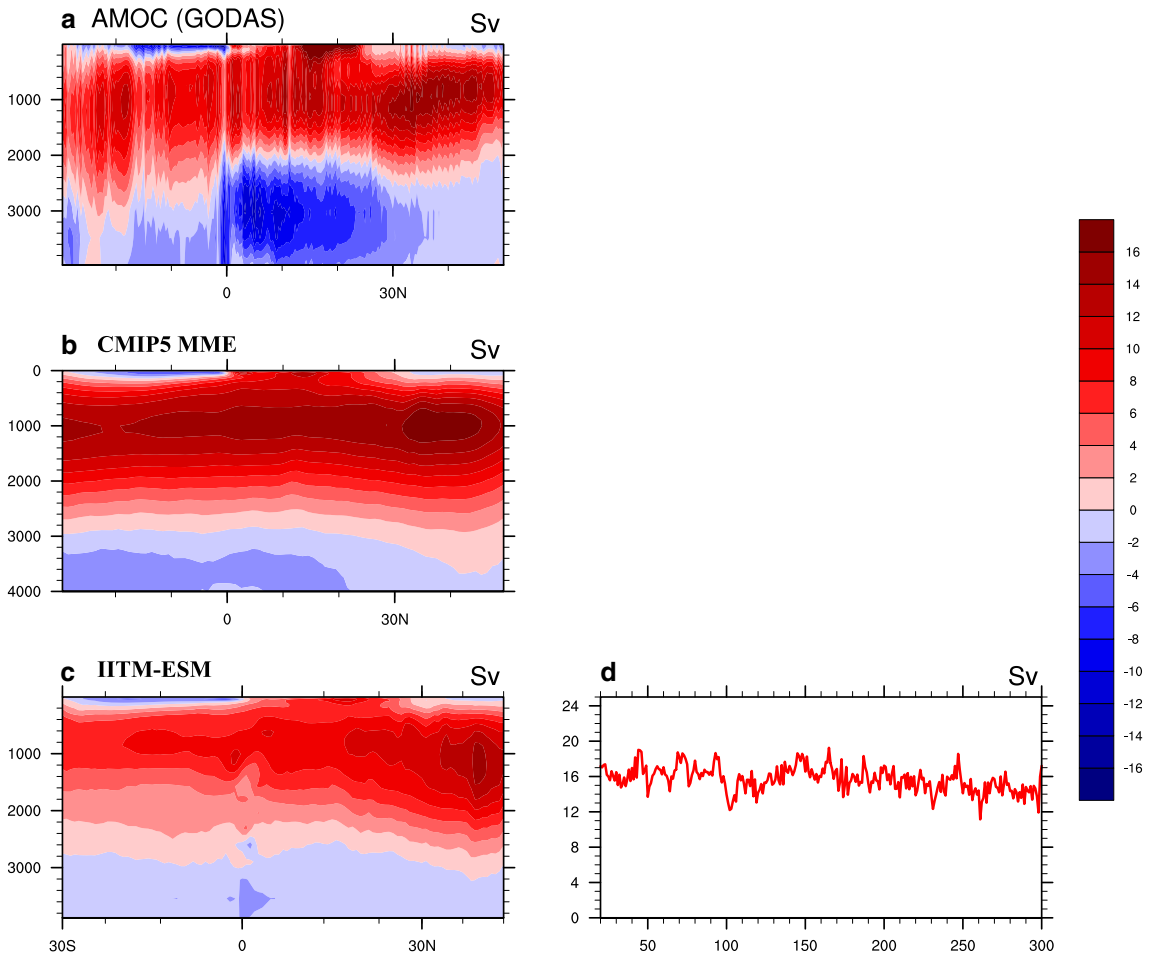

Fig. 2 Latitude-depth section showing Atlantic Meridional Overturning Circulation (AMOC, Sv) from (**a**) GODAS, (**b**) CMIP5 ensemble mean, and (**c**) Pi-Control of IITM-ESM. **d** Time series of maximum AMOC transport (Sv) in the north Atlantic from preindustrial simulation of IITM-ESM

15.8 Sv, while the observational estimate of the AMOC at 26.5^0 N is 18.5 Sv (Johns et al. 2008; Kanzow et al. 2010b; Trenberth and Fasullo 2017). The vertical-meridional pattern of AMOC is well represented in the model. Though the magnitude of the simulated AMOC is slightly weaker than the observations, the mean features are reasonably well simulated by the model as compared to observations and CMIP5 multi-model mean.

4.2 South Asian monsoon characteristics in IITM-ESM

An assessment of the mean monsoon characteristics over the South Asian region during boreal summer monsoon season (June–September; hereafter JJAS) from the piControl simulation of IITM-ESM, satellite-derived TRMM data, and CMIP5 multi-model mean, are shown in Fig. 3. The mean rainfall during JJAS is characterized by rainfall over central India and the surrounding parts of the Arabian Sea and the Bay of Bengal with the rain belt extending to the Maritime Continent and across the Pacific Ocean between the equator and 10^0 N (Fig. 3a). IITM-ESM reproduces the observed precipitation pattern reasonably well. The IITM-ESM shows a dry bias over the Amazon region, Southeast Asia and equatorial Pacific, while dry bias over Indian region and excess rainfall bias over the western Pacific is reduced in the current version as compared to the previous version of IITM-ESM (Swapna et al. 2014, 2018a). The current version of IITM-ESM employs a new parameterization scheme, Revised Simplified Arakawa Schubert (SAS) scheme (Han and Pan 2011) which resulted in a better simulation of rainfall over the tropical region (Ganai et al. 2015; Swapna et al. 2018b). In the revised SAS scheme, the cumulus convection is made stronger and deeper to deplete more instability in the atmospheric column. More details about the revised SAS scheme are available in Han and Pan (2011).

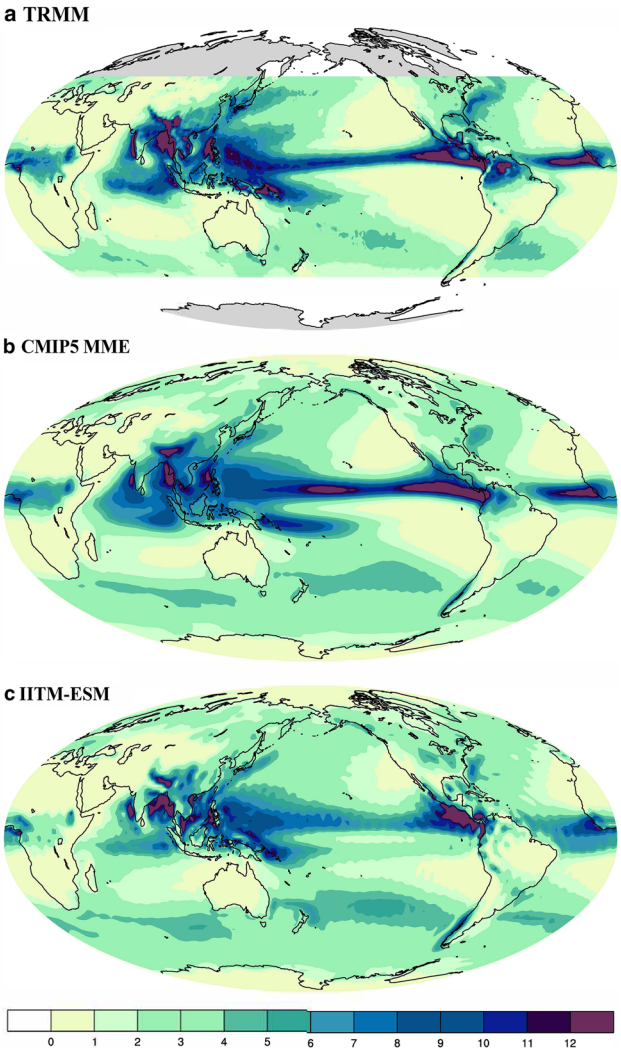

Fig. 3 Spatial map of boreal summer monsoon (JJAS) precipitation (mm d^{-1}) from (**a**) Observation (TRMM), (**b**) CMIP5 ensemble mean and (**c**) IITM-ESM

5 Simulated changes in the AMOC and South Asian monsoon in a warming climate

The CMIP5 models project a significant decline in the strength of AMOC in the 21st century. A suite of studies were performed to evaluate the response to the declining strength of AMOC strength using idealized experiments. Stouffer et al. (2006) performed a freshening experiment in which they distributed 1.0 Sv of freshwater into the entire northern North Atlantic. They observed that the AMOC weakens rapidly and almost disappears in most models and as a result, poleward heat and salt transport in the north Atlantic reduce dramatically. Consequently, the Northern Hemisphere (NH) cooled and the Southern Hemisphere (SH) warmed relative to the control simulation. The magnitude of NH cooling was much greater than the SH warming. As a result, the annual mean Atlantic ITCZ moved into the Southern Hemisphere. Similarly, Zhang and Delworth (2005), Sun et al. (2011) also have performed idealized freshening experiments and established the association between AMOC and ITCZ location.

However, future changes in the large-scale global climate driver AMOC and its possible association with regional monsoon-like South Asian monsoon in a warming climate have not yet been addressed. In the current study, we propose a mechanism linking the unprecedented decline of AMOC (by imposing surface heat flux) to the weakening of monsoon circulation in a warming climate.

In order to understand the association between AMOC and large scale monsoon circulation in a warming climate, we perform a series of sensitivity experiments using the IITM-ESM. The experiments are performed under the FAFMIP (Gregory et al. 2016b) protocol. The details about the experiments are listed in Table 1. These experiments help in classifying the role of weakening of large scale thermohaline circulation alone on the South Asian monsoon amidst a plethora of factors viz GHG and anthropogenic aerosols. Here, we analyze the simulation characteristics from FAF-HEAT and FAF-WATER experiments, in which heat and freshwater flux anomalies are added as forcing, keeping all other parameters unchanged from the piControl following the FAFMIP protocol (Gregory et al. 2016b).

5.1 Response of AMOC to anomalous heat and freshwater forcing

The AMOC streamfunction from the FAFMIP experiments is shown in Fig. 4. Figure 4a shows the mean AMOC structure from the piControl simulation. Figure 4b and c show the changes in AMOC represented as the difference between FAF-HEAT and piControl (Fig. 4b) and FAF-WATER and piControl (Fig. 4c) respectively. The last 10 years from each experiment are considered for the analysis. Though both the experiments show a weakening of AMOC, the strength is considerably decreased in FAF-HEAT. This can also be seen from the time series of maximum AMOC stream function from both the experiments and piControl shown in Fig. 4e. The magnitude of the decline in AMOC from FAF-HEAT and FAF-WATER is similar to the decline shown by CMIP5 models under FAFMIP experiment (Gregory et al. 2016b). Since FAF-HEAT has a larger impact on the decline of AMOC, we focus on FAF-HEAT results for further analysis. It was also shown by previous studies that surface heat flux anomalies have a dominant influence on the AMOC variability (Rahmstorf and Ganopolski 1999; Mikolajewicz and Voss 2000; Gregory et al. 2005). Also, we see a decline of AMOC in a transient CO_2 simulation which will be further discussed in detail in the subsequent section (Fig. 4d).

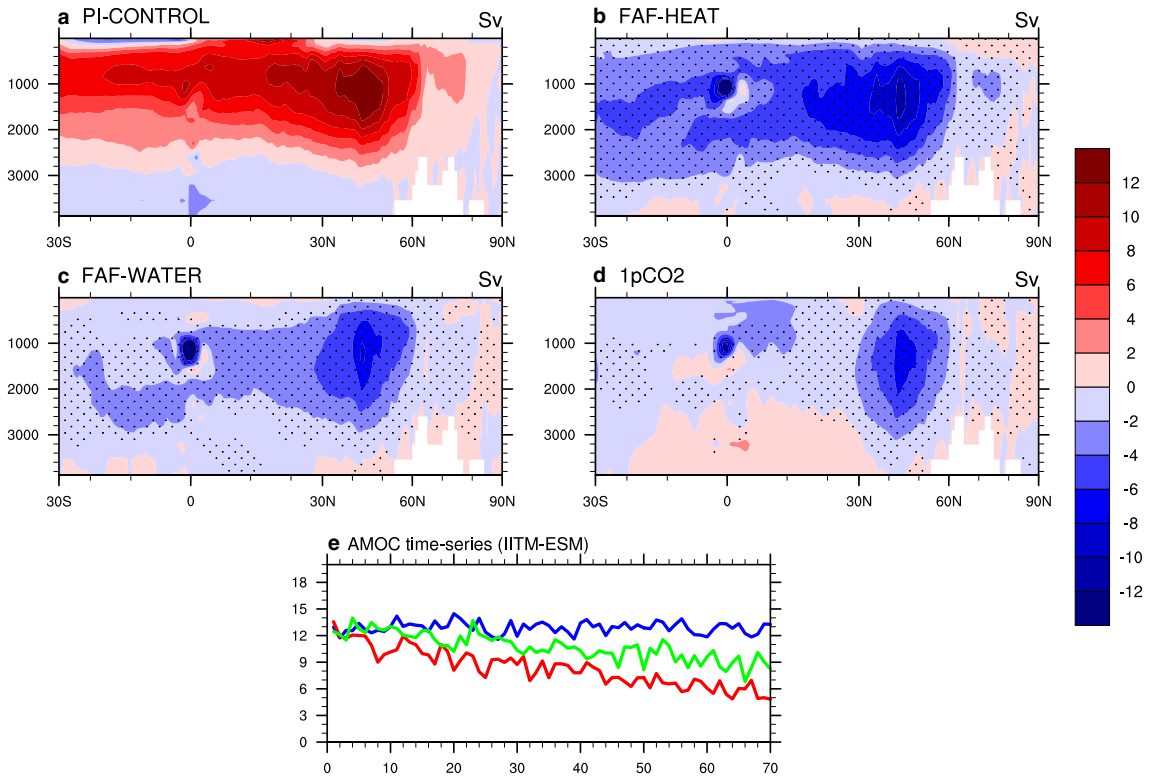

Fig. 4 Latitude-depth section showing mean Atlantic Meridional Overturning Circulation (AMOC, Sv) from (**a**) piControl, relative to piControl from (**b**) FAF-HEAT (**c**) FAF-WATER and (**d**) 1 pct CO2. **e** Time series of maximum AMOC transport (Sv) in the north Atlantic from piControl (blue), FAF-HEAT(red) and FAF-WATER(green). Change in the AMOC significant at 95% confidence interval are stippled

In order to understand the possible reasons for the decline of AMOC, we analyze the annual mean sea-ice concentration over the Arctic (Fig. 5). Figure 5a shows the annual mean sea-ice concentration over the Arctic from the piControl. Figure 5b shows the difference of the arctic sea-ice concentration from FAF-HEAT relative to piControl. We clearly see a decline in the sea-ice concentration in FAF-HEAT experiment (Fig. 5b). The depletion of Arctic sea-ice results in the discharge of fresh water into the North Atlantic.

Further, we analyze the meridional-vertical profiles of temperature and salinity in the Atlantic basin (Fig. 6). Figure 6 shows the mean vertical-meridional Atlantic salinity profile from the piControl and difference from FAF-HEAT relative to piControl. We observe a freshening relative to piControl in FAF-HEAT (Fig. 6c) which is a result of discharge of fresh water from the Arctic sea-ice melt. We also observe an increase in the temperature relative to piControl in FAF-HEAT due to the net positive surface heat flux anomaly forcing (Fig. 6d). Changes in salinity affect buoyancy and density stratification in the North Atlantic and play an important role in controlling the strength of meridional overturning circulation (Buckley and Marshall 2016). The excessive freshening in the North Atlantic can be caused by the depletion of sea-ice in the Arctic (Sévellec et al. 2017; Liu and Fedorov 2019) or through the land-ice melt over Greenland (Rahmstorf et al. 2015). Since freshening arising from the land-ice melt is not included in both these experiments, the excessive freshening can only be induced by the changes in the sea-ice distribution alone.

To gain further insight, we also analyze the potential density (averaged over upper 500 m) in the Atlantic basin from piControl and FAF-HEAT (Fig. 7). A basin-wide decrease in the potential density in the North Atlantic can be seen in FAF-HEAT relative to piControl (Fig. 7b) resulting from increased warming and freshening arising from the anomalous heat flux forcing.

5.2 Response of South Asian monsoon to anomalous weakening of AMOC

In this section, we analyze the impacts of the weakening AMOC to changes in large-scale circulation and precipitation patterns over the South Asian region. There are compelling evidences from recent studies that weakening of the AMOC has a central role in weakening the northward oceanic heat transport and shifting the position of the ITCZ (McGee et al. 2014, 2018). Also, AMOC fluctuations affect the strength of the mean atmospheric tropical

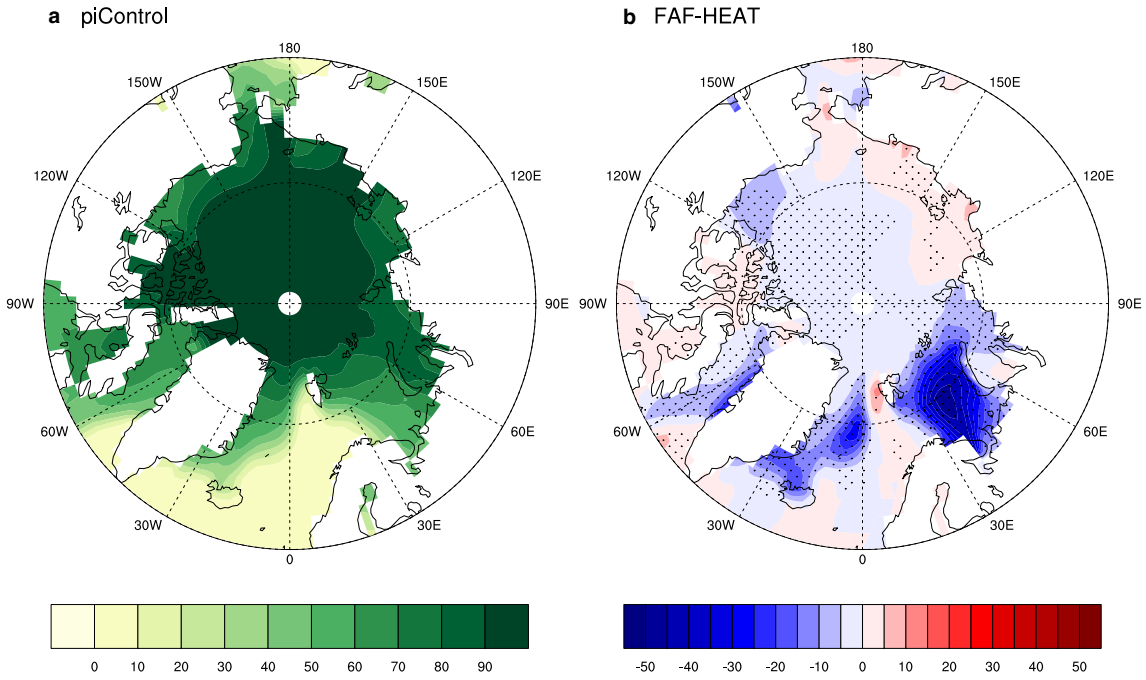

Fig. 5 Spatial map of annual mean sea-ice concentration (%) over the Arctic from (**a**) piControl, (**b**) relative to piControl from FAF-HEAT. Changes in Sea-ice significant at 95% confidence level are stippled

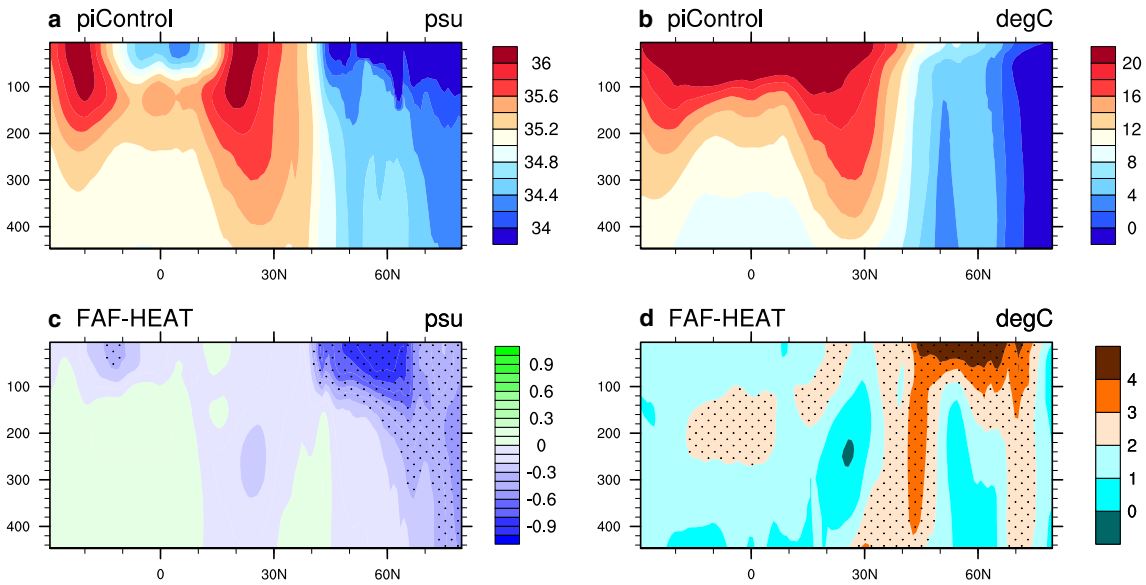

Fig. 6 Latitude-depth section of upper layers of mean Atlantic salinity (psu) from (**a**) piControl, relative to piControl from (**c**) FAF-HEAT. (**b**, **d**) similar to (**a**, **c**) except for potential temperature (°C). Changes in the temperature and salinity significant at 95% confidence level are stippled

circulation by impacting global atmospheric energetics (Vial et al. 2018). Further, we analyze the poleward ocean heat transport (OHT) from the experiments. The poleward OHT is shown in Fig. 8. Figure 8a shows the mean poleward heat transport from both Ocean and Atmosphere from piControl. It is interesting to note that there is a considerable decline in the Atlantic OHT in FAF-HEAT associated with a weakening of AMOC in the experiment (Fig. 8b). The reduction of OHT is associated with a cooling in the Northern hemisphere (NH) and warming in the Southern hemisphere. The SST difference from both FAF-HEAT and 1 pct CO_2 relative to piControl is shown

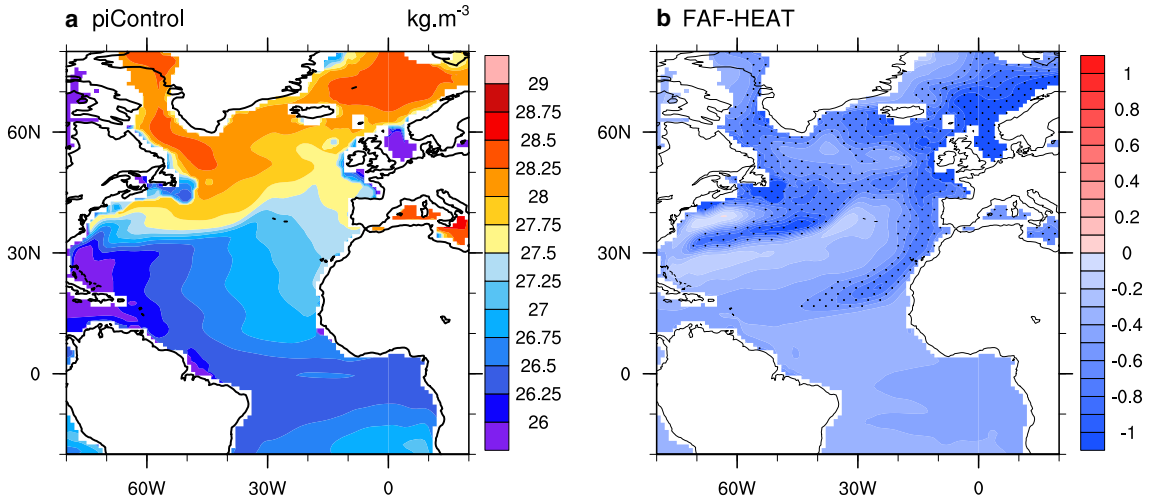

Fig. 7 Spatial map showing the mean north Atlantic potential density (kg m^{-3}) from (**a**) piControl, (**b**) relative to piControl from FAF-HEAT. Change in potential density significant at 95% confidence level are stippled

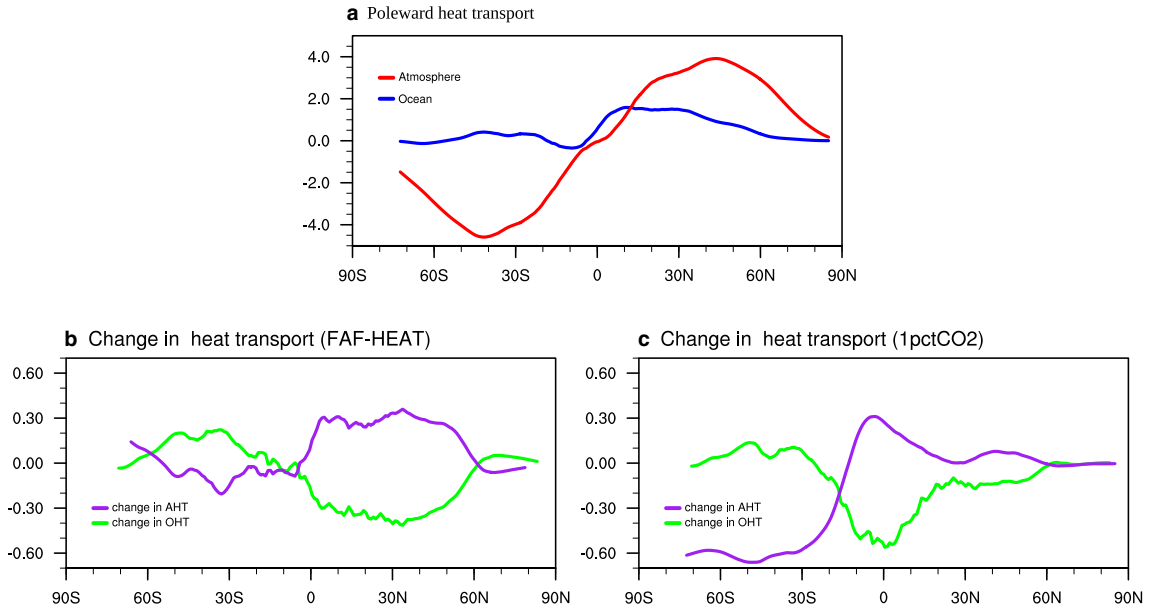

Fig. 8 **a** Annual mean cross-equatorial heat transport (PW) from piControl, Ocean (blue), Atmosphere (red) (**b**). Change in the ocean heat transport (green), change in the atmospheric heat transport (purple) relative to piControl from FAF-HEAT (**c**). Change in the ocean heat transport (green), change in the atmospheric heat transport (purple) relative to piControl from 1 pct CO_2

in Fig. 9. In FAF-HEAT, we observe a north–south temperature gradient with cooling in the northern hemisphere and warming in the southern hemisphere (Fig. 9a). This inter-hemispheric SST difference in-turn leads to a southward shift of the ITCZ, as ITCZ is located in the warmer hemisphere (Mantsis and Clement 2009; Donohoe et al. 2013; Sun et al. 2013; Haywood et al. 2016). Associated with the weakening of large-scale north–south temperature gradient, the regional land-sea thermal gradient has also weakened as can be seen from Fig. 10 for the summer monsoon season.

It is well known that the land-sea thermal contrast can modulate the regional monsoon circulation (Sikka and Gadgil 1980; Lau and Li 1984; Li and Yanai 1996; Webster et al. 1998; Rajeevan et al. 2010). Since Indian summer monsoon typically lasts from June to September season (JJAS) bringing more than 90% of the total precipitation, we further analyze the fields for the JJAS. Land-sea thermal

contrast over the South Asian region is computed based on the method discussed by Xavier et al. (2007). Land-sea thermal contrast is defined as the temperature averaged from 850 to 200 hPa has a strong influence on the South Asian summer monsoon rainfall. We show the summer mean temperature (averaged from 850 to 200 hPa) from piControl in Fig. 10a. Figure 10b shows the weakening of the land-sea thermal gradient from FAF-HEAT relative to piControl. Weakening of the land-sea thermal gradient weakens the Sea level Pressure (SLP) gradient (Fig. 11) and regional Hadley cell during the summer monsoon season (Fig. 12). Figure 11a shows the mean SLP during the summer season from the piControl. Figure 11b shows the weakening of SLP gradient from FAF-HEAT relative to piControl. Also, since large-scale South Asian summer monsoon circulation has a strong linkage to the changes in the Hadley cell, we analyzed regional Hadley cell during the summer season. Figure 12a shows the mean Hadley cell from piControl, comprising of an ascending branch over the Indian landmass and a descending branch over the equatorial Indian Ocean. Figure 12b shows a descent over the Indian land region and rises over the equatorial Indian Ocean associated with weakening

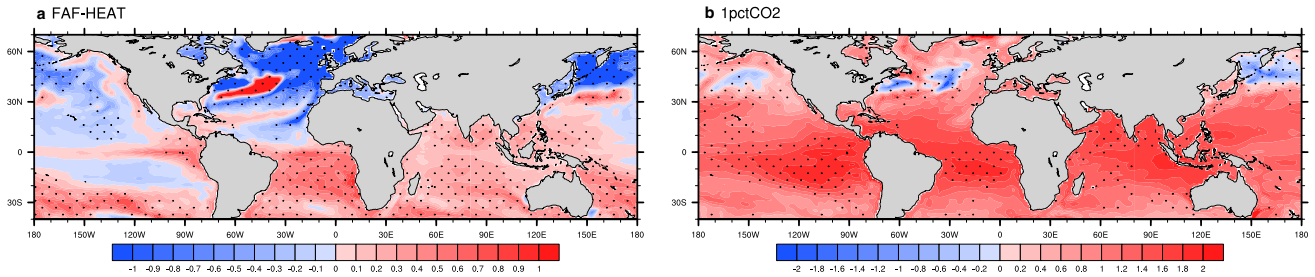

Fig. 9 Spatial map showing the difference in Sea Surface Temperature (°C) relative to piControl from (**a**) FAF-HEAT and (**b**) 1 pct CO_2. Changes in SST significant at 95% confidence interval are stippled

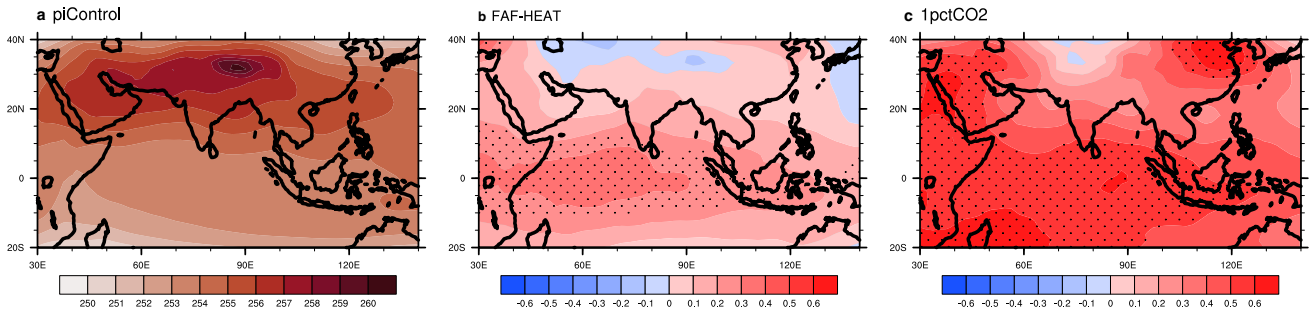

Fig. 10 JJAS seasonal mean temperature (K, averaged from 850 to 200 hPa) from (**a**).piControl, relative to piControl from (**b**) FAF-HEAT and (**c**) 1 pct CO2. Change in temperature significant at 95% confidence level are stippled

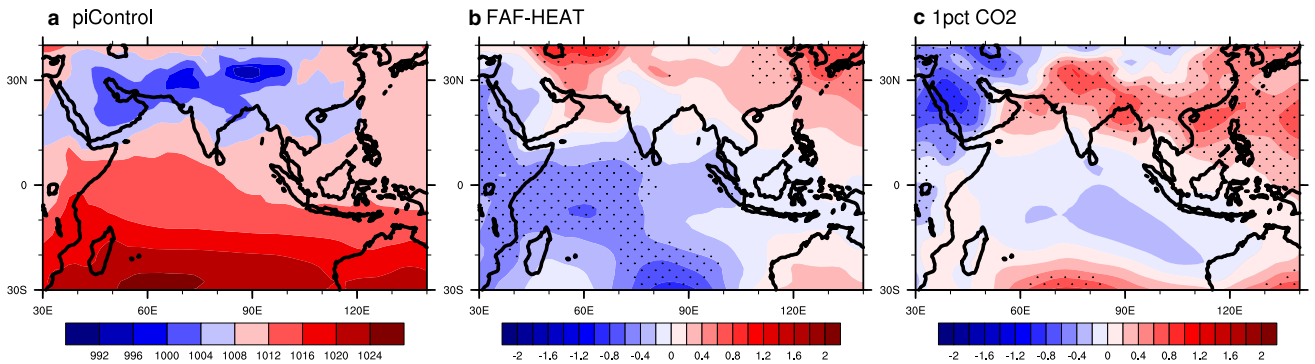

Fig. 11 **a** Spatial map of JJAS mean Sea Level Pressure (MSLP,hPa) from (**a**). piControl, relative to piControl from (**b**) FAF-HEAT and (**c**). 1 pct CO2. Change in MSLP significant at 95% confidence interval are stippled

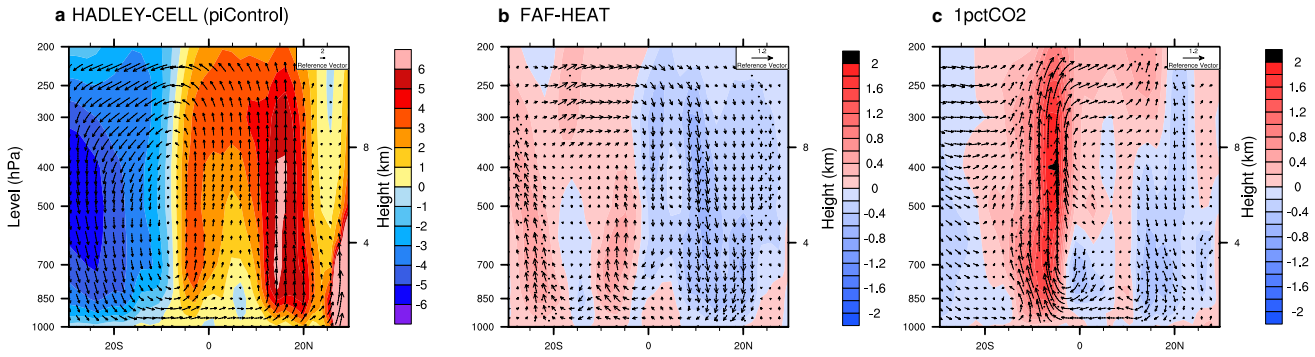

Fig. 12 Meridional–vertical profile of JJAS seasonal mean circulation (Hadley Cell) averaged over 65°E–95°E (vectors), vertical velocity (10^{-4} Pa s^{-1}) (shaded) from (**a**). piControl, (**b**). Relative to piControl from FAF-HEAT. **c** 1 pct CO2. Changes in the vertical velocity significant at 95% confidence level are stippled

of regional Hadley cell from FAF-HEAT relative to piControl. Since weakening of the summer monsoon Hadley cell can potentially lead to a weakened large-scale monsoon flow, we further evaluate the monsoon features.

The mean summer monsoon rainfall from the piControl and FAF-HEAT is shown in Fig. 13a–d. The 850hpa cross-equatorial vector winds were overlaid in order to diagnose the monsoon circulation response. Figure 13a shows the climatology of the precipitation and winds from piControl, while Fig. 13c shows the difference from FAF-HEAT relative to piControl. The change in circulation and precipitation from FAF-HEAT over the South Asian region is shown in Fig. 13b and d. We note that with the weakening of summer mean Hadley circulation co-occurring with the weakening of AMOC, summer monsoon circulation and precipitation over South Asian region also have shown a considerable decline.

In summary, the decline in the strength of AMOC can be one of the factors for the changes in the large-scale circulation pattern. AMOC decline weakens the poleward OHT, causing a meridional thermal gradient by cooling the NH and warming the SH. This thermal gradient shifts the ITCZ to the SH. The weakened large-scale summer mean Hadley cell weakens the cross-equatorial monsoon circulation and precipitation. But, in a realistic future warming scenario, increasing concentrations of GHG's have been known to increase moisture availability and precipitation (Stowasser et al. 2009). Therefore, in the next section, we analyze the changes in the South Asian monsoon from the perspective of a declining AMOC under an increasing CO_2 scenario.

6 Projected changes in the association between AMOC and South Asian Monsoon

Understanding the South Asian monsoon response to global warming is a challenging problem (Turner and Annamalai 2012). CMIP3 future projections of ISMR revealed a wide range of trends with varying magnitudes. An evaluation of ISMR from 20 CMIP5 models for the period 1850 to 2100 showed a consistent increase in seasonal mean rainfall (Menon et al. 2013). The long-term positive trends in the monsoon rainfall and interannual variability is a robust feature across a wide range of models (Kripalani et al. 2007; Hsu et al. 2013; Lee and Wang 2014). However, summer monsoon circulation is projected to decline under global warming (Kitoh et al. 1997; Tanaka et al. 2005; Ueda et al. 2006).

The increase in precipitation under global warming is attributed to an increase in the water-holding capacity of the atmosphere with an increase in surface temperature (Trenberth 1998). Meehl et al. (2005) suggested an increase in water vapor content associated with an increase in sea surface temperature in a warmer climate as the reason for enhanced precipitation in the tropics. The atmospheric water vapor is projected to increase by 12–16% over large parts of India (Kripalani et al. 2007) at the time of CO_2 doubling. This increase in moisture content can lead to enhanced precipitation.

In order to understand the association between AMOC and South Asian monsoon in a warming scenario, we have performed an idealized future warming scenario experiment by increasing CO_2 at a rate of 1% per year (1 pct CO_2) until doubling (Taylor et al. 2012). Figure 4d shows the AMOC strength from 1pctCO_2 relative to piControl. We observe a decline in the AMOC strength with an increase in CO_2, AMOC strength declined by almost 5.0 Sv at the time of doubling CO_2. The AMOC weakening is larger in FAF-HEAT than in 1pctCO_2 which is consistent with the four AOGCMs used in Gregory et al. (2016b).

Similar to Sect. 5, we analyze the OHT changes from 1pctCO2. We find a decline in poleward OHT in 1 pct CO_2 similar to FAF-HEAT (Fig. 8c). The SST difference from 1pctCO2 relative to the piControl (Fig. 9b), shows enhanced SST warming with relatively higher warming

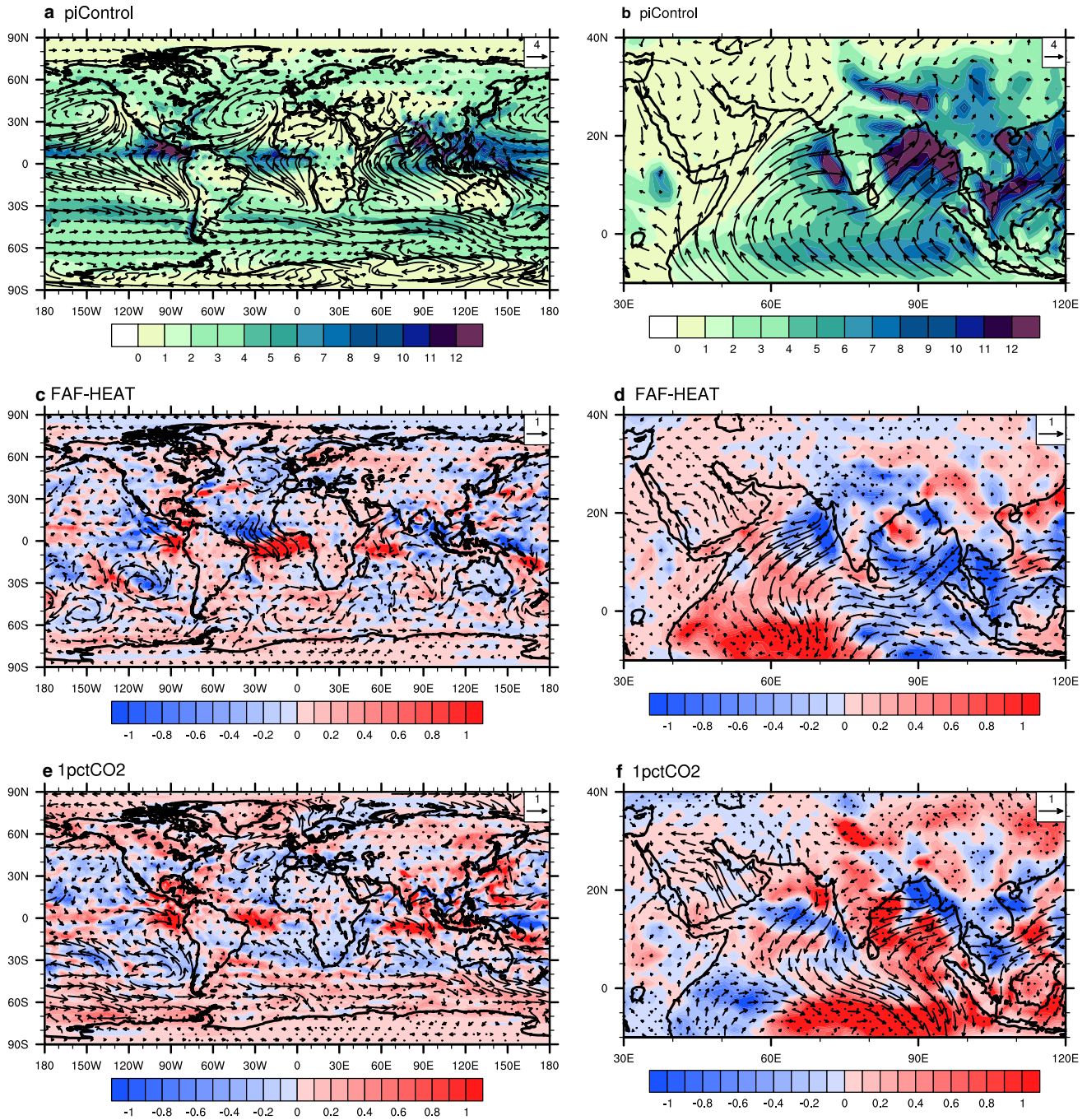

Fig. 13 **a** Spatial map showing the boreal summer (JJAS) mean precipitation (shaded, mm d^{-1}), 850 hPa wind (vectors, m s^{-1}) overlaid from piControl (**b**) same as (**a**) but zoomed Over South Asian region, relative to piControl (**c**) from FAF-HEAT, (**d**). Same as (**c**) but zoomed Over South Asian region, relative to piControl (**e**) from 1pctCO_2, (**f**). Same as (**c**) but zoomed Over South Asian region. Change in the precipitation significant at 95% confidence level are stippled

in the equatorial Indian Ocean as compared to the northern regions. Though global warming is generally spatially uniform, we see a weaker north–south SST gradient in 1 pct CO_2 compared to FAF-HEAT. The enhanced warming in the equatorial Indian Ocean weakens the land-sea thermal gradient similar to FAF-HEAT (Fig. 10c). Weakening of the land-sea thermal gradient weakens the SLP gradient and regional Hadley cell. The SLP, regional Hadley cell and South Asian monsoon circulation from 1pctCO2 also show a weakening similar to FAF-HEAT (Figs. 11c, 12c). Thus both the FAF-HEAT and 1 pct CO_2 experiment reveal a weakening of summer monsoon circulation over

the South Asian region associated with the weakening of AMOC.

Summer monsoon circulation and precipitation response from 1 pct CO_2 is shown in Fig. 13. We note the difference in precipitation and circulation response in 1 pct CO_2 as compared to FAF-HEAT (Fig. 13f). An increase in the summer monsoon precipitation over the south Asian region despite the weakening of the cross-equatorial flow can be seen from Fig. 13f in contrast to the FAF-HEAT where weakening of both circulation and precipitation can be seen over the south Asian region (Fig. 13d).

We further diagnose the difference in the precipitation response between FAF-HEAT and 1 pct CO_2 despite a common decline in AMOC in both experiments. To gain further understanding, we decompose the thermodynamic and dynamic contribution to monsoon circulation and precipitation changes.

6.1 Thermodynamic and dynamic contribution to monsoon circulation and precipitation changes

Under global warming, the increase in precipitation has been attributed predominantly to an increase in the water-holding capacity of the atmosphere with an increase in surface temperature (Trenberth 1998). This may be the reason for the increase in the monsoon precipitation despite weakening of monsoon circulation in the 1 pct CO_2 experiment. The general hypothesis is that, in a warmer climate, based on the Clausius–Clapeyron equation, surface evaporation will increase with increasing SST, and this additional moisture content in the troposphere results in excess rainfall (Stowasser et al. 2009). Because in all FAFMIP experiments the CO_2 concentrations were prescribed at the pre-industrial level, the water-holding capacity of the atmosphere is less in the FAF-HEAT experiment as compared to 1pct CO_2 experiment.

Idealized aqua-planet simulations clearly demonstrate that low-level moisture transport in the atmospheric Hadley cell opposes the atmospheric energy transport (Frierson et al. 2013; Voigt et al. 2013; Haywood et al. 2016). We analyze the 850 hPa moisture flux (g kg^{-1} m s^{-1}) and lower troposphere (850–500 hPa) integrated moisture (g kg^{-1}) from both 1 pct CO_2 and FAF-HEAT relative to piControl (Fig. 14). We see a weakening of 850 hPa moisture flux into the South Asian region in the FAF-HEAT relative to piControl (Fig. 14a). In contrast, the 1 pct CO_2 shows an enhancement of 850 hpa moisture flux implying an increase of moisture flux (Fig. 14b). An enhancement of vertically integrated moisture can be seen in 1 pct CO_2, while there is no significant change in moisture in the FAF-HEAT (Fig. 14c, d). Further, we evaluate moisture divergence from both the experiments. Figure 14e shows a divergence of moisture over the landmass in FAF-HEAT and convergence of moisture in the 1 pct CO_2 (Fig. 14f). This confirms that the enhancement of precipitation seen in 1 pct CO_2 is due to the excess of moisture availability as compared to FAF-HEAT.

Further, we also decompose the rainfall change into thermodynamic and dynamic components based on Huang et al. (2013). Following the equation $P' \sim w' \times q + w \times q'$; we split the water vapor budget into dynamic and thermodynamic components. The first component from the equation derived from Huang et al. (2013) is the dynamic component which represents the changes in the circulation. The second component is the thermodynamic component which represents the change in the water vapor due to warming. The thermodynamic effect due to global warming plays a dominant role in the 1 pct CO2 in contrast to FAF-HEAT. Figure 15b and d show the thermodynamic component from FAF-HEAT and 1pctCO2 respectively. In FAF-HEAT, the net surface heat flux anomaly is used as the only forcing. The GHG concentrations were kept constant in FAF-HEAT. Therefore the q' (i.e. the change in specific humidity) is minimal in FAF-HEAT. The thermodynamic component (i.e. second term) is not significant and hence not have strong impact on the rainfall as can be seen from (Fig. 15b and d).

In 1 pct CO_2, the CO_2 concentration is increased at a rate of 1% per year. As the CO_2 concentration increases, the temperature increases and the water holding capacity of the atmosphere increases. Therefore q' (i.e. change in specific humidity) is substantial in 1pctCO2 relative to piControl. Therefore the thermodynamic component is significant in 1pctCO2 leading to moisture convergence and enhanced rainfall over south Asian region. In addition, we show the vertically integrated moist static energy (MSE) from both FAF-HEAT and 1 pct CO_2 (Fig. 14). We find an increase in the MSE in 1 pct CO_2 owing to the enhanced availability of moisture, which confirms the increase in the thermodynamic component. The dynamic contribution is largely consistent with FAF-HEAT. This explains the contrasting rainfall features in the FAFHEAT and transient CO_2 experiments.

In summary, the numerical experiments performed with IITM-ESM show consistent results of weakening summer monsoon circulation over the South Asian region with a decline of AMOC, though precipitation response is dominated by the thermodynamics response in a GHG warming scenario.

7 Conclusions

In this work, we focused on the association between AMOC and South Asian monsoon in a warming climate. Long term proxy records (1200 years from 800 to 2000AD) of AMOC and ISMR showed a close relationship. During periods of

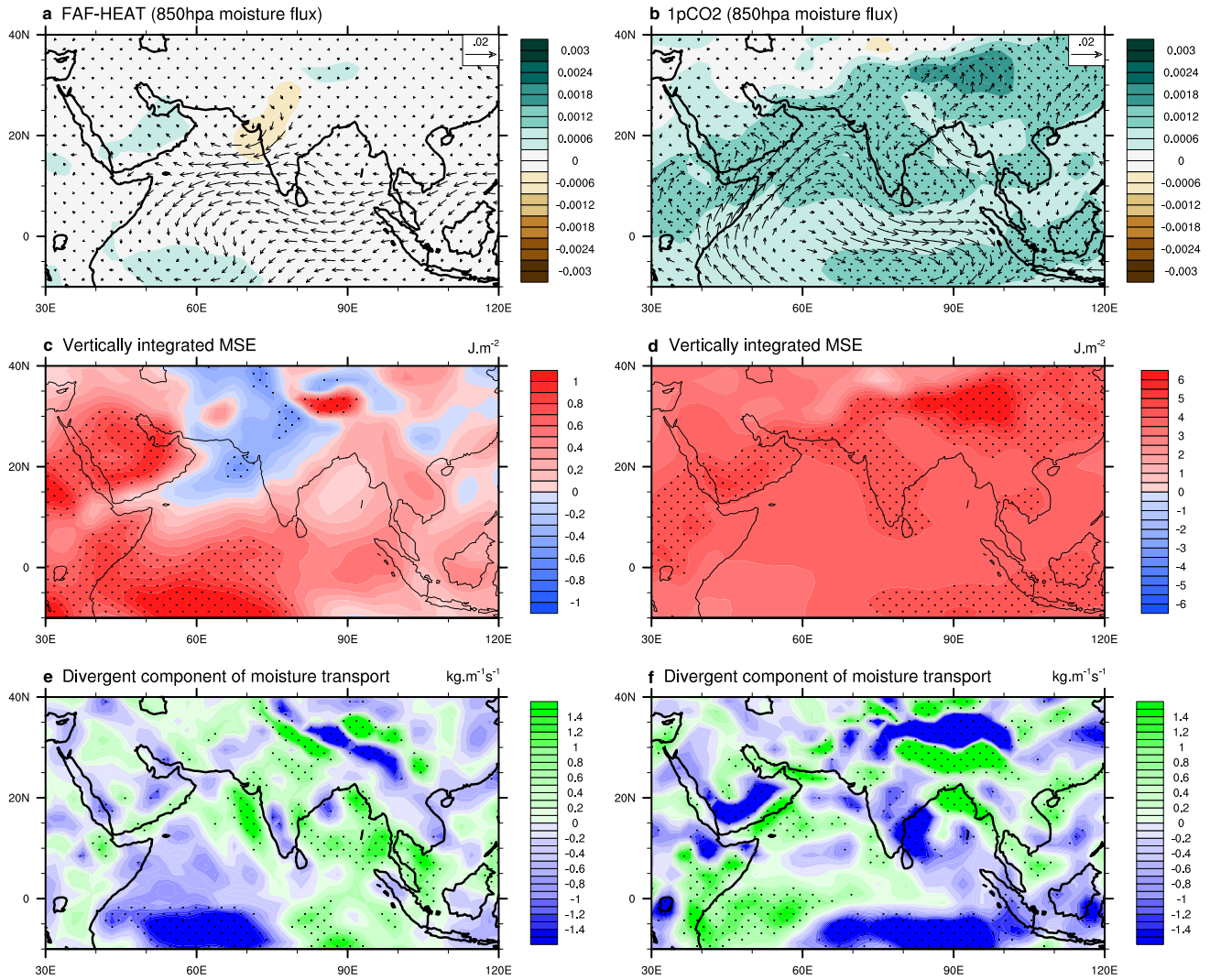

Fig. 14 Seasonal mean (JJAS) difference of FAF-HEAT and 1pctCO2 relative to piControl (**a**) moisture flux at 850 hPa (vectors, g kg^{-1} m s^{-1}) over specific humidity at 850 hPa (shaded), **c** 1000–700 hPa vertically integrated moist static energy (J m^{-2}). **e** Divergent component of moisture transport (kg m^{-1} s^{-1}) (**b**, **d**, **f**) same as (**a**, **c**, **e**) but for 1 pctCO_2. Changes significant at 90% confidence level are stippled

weak AMOC, ITCZ shifts southward and ISMR is characterized by reduced precipitation. Observational records indicate a twentieth-century slowdown in AMOC and CMIP5 models project an AMOC decline of more than 30% under the extreme scenario of RCP8.5 at the end of the 21st century (Kirtman et al. 2013). In the background of global warming and projected weakening of AMOC, we explored the links between the projected unprecedented decline in the strength of AMOC and its impact on the circulation and precipitation patterns over the South Asian region using IITM-ESM CMIP6 and sensitivity experiments. Understanding the circulation and precipitation changes to a substantial decline in AMOC as projected by CMIP5 models is vital given that nearly half of the world's population in the South Asian region heavily relies on monsoon for agriculture, food, and energy security.

An assessment of the IITM-ESM model simulations of AMOC and South Asian monsoon was performed. The model captures the mean characteristics of AMOC and South Asian monsoon in the piControl simulation. Sensitivity experiments performed with IITM-ESM revealed a significant association between South Asian Monsoon circulation and AMOC. While previous studies have already reported an association between AMOC and South Asian monsoon, projected changes in AMOC and its possible influence on the regional South Asian monsoon in a warming climate have not yet been addressed.

To understand the responses of the large-scale circulation and precipitation to a substantial AMOC weakening, a series of experiments were performed. Model experiments performed with realistic surface heat and freshwater perturbations, derived from the Flux Anomaly Forcing

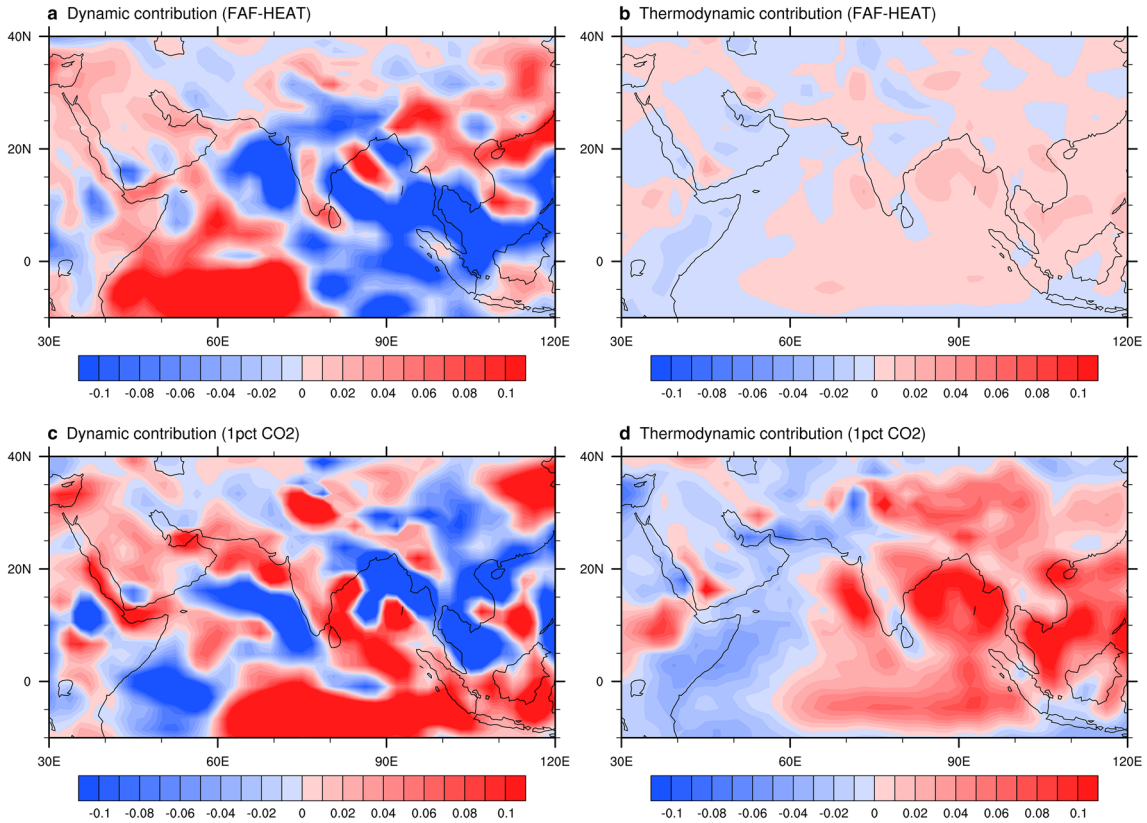

Fig. 15 Decomposition of precipitation change, **a**–**d**. **a** Dynamic (10^{-4} Pa s^{-1}). **b** Thermodynamic component (10^{-4} Pa s^{-1}) of rainfall change for FAF-HEAT. **c** Dynamic (10^{-4} Pa s^{-1}) and **d** thermodynamic (10^{-4} Pa s^{-1}) component of rainfall change for 1 pct CO_2

Model Intercomparison Project (FAFMIP; Gregory et al. 2016a), revealed a decline in the strength of AMOC which leads to regional and remote responses. When imposing the surface heat flux anomalies (FAF-HEAT), the AMOC declined significantly in response to the surface heat added into the North Atlantic. The weakening of AMOC results in the reduction of northward oceanic heat transport and an enhanced northward atmospheric heat transport and weakening of large-scale north–south temperature gradient. This in-turn weakens the regional land-sea thermal gradient, regional Hadley circulation, monsoon circulation and precipitation over the South Asian region. In addition, we also performed a surface freshwater flux anomaly experiment (FAF-WATER). As in previous studies, we find surface heat flux perturbations (i.e. FAF-HEAT) to play a dominant role in the AMOC decline (Gregory et al. 2016a, b; Delworth et al. 1993; Griffies and Tziperman 1995; Delworth and Greatbatch 2000).

Finally, in order to understand the association between AMOC and monsoon in a warming climate, we performed an additional experiment in which we increased the CO_2 concentration at the rate of 1% per year, and found that circulation responses are similar to FAF-HEAT and robust. We find the magnitude of weakening of AMOC in transient CO_2 to be weaker than in FAF-HEAT, which is consistent with previous studies. It is interesting to note that though the South Asian monsoon circulation responds to the weakening of AMOC, precipitation responses are different An enhancement of precipitation results from the transient CO_2 experiment despite a weakening of summer monsoon circulation. Precipitation changes are dominated by the thermodynamic response leading to enhancement of precipitation over the south Asian region. Our diagnostics imply that, in addition to the increase in CO_2-induced rise in temperature, there is increased availability of moisture and moist static stability. The changes in moisture flux led to increased South Asian summer monsoon precipitation.

There are two novel aspects in the current study. Firstly, we distinguish the process of AMOC weakening quantitatively by imposing surface heat fluxes (FAF-HEAT) and fresh water fluxes (FAF-WATER) individually. We find an enhanced weakening of AMOC in FAF-HEAT rather than FAF-WATER experiment indicating the importance of the heat flux on AMOC weakening. Most of the previous studies were assessing the impact of freshening on AMOC weakening. These studies discussed the association between weakening of the AMOC and South Asian monsoon using idealized experiments by inducing freshening in the North

Atlantic. However, heat flux variations have a dominant influence on AMOC variability (Delworth et al. 1993; Griffies and Tziperman 1995; Delworth and Greatbatch 2000). Here for the first time, we used heat flux anomaly to weaken the AMOC and studied the association between declining AMOC and South Asian monsoon. For this, we followed the FAFMIP protocol, in which we impose the net surface heat flux anomaly i.e. FAF-HEAT.

The second novel aspect of our study is with a suite of experiments we demonstrate that the South Asian monsoon circulation weakens in response to weakening AMOC, while precipitation changes are dominated by thermodynamics response. To demonstrate the association between AMOC and South Asian monsoon in a warming climate we performed a 1p CO_2 experiment in which CO_2 concentration is increased at a rate of 1% per year. We find a decline in the strength of AMOC in 1p CO_2 similar to FAF-HEAT. South Asian circulation weaken in response to AMOC weakening in both FAF-HEAT and 1p CO_2 experiment. However, the South Asian monsoon precipitation response is distinct in 1p CO_2 experiment. We investigated the difference in the precipitation response from both the experiments by performing water budget analysis. Our results reveal that the thermodynamic component of the water vapor budget plays a major in driving the South Asian monsoon precipitation in a future warming scenario in spite of a decline in the strength of AMOC.

Acknowledgements We thank Director, IITM for extending full support for this research. The IITM-ESM simulations were performed on the IITM HPC Aaditya. IITM receives full support from the Ministry of Earth Sciences, Government of India. Author SN acknowledges the STEP program, ICTP, Italy. A part of the experiments and analysis was carried out at ICTP, Italy as a part of the STEP program. Freeware Ferret and NCL are used for the analysis of model simulations. All data sources are duly acknowledged.

References

Altabet MA, Higginson MJ, Murray DW (2002) The effect of millennial-scale changes in Arabian Sea denitrification on atmospheric CO2. Nature 415:159–162

Belkin IM, Levitus S, Antonov J, Malmberg SA (1998) "Great salinity anomalies" in the North Atlantic. Prog Oceanogr. https://doi.org/10.1016/S0079-6611(98)00015-9

Buckley MW, Marshall J (2016) Observations, inferences, and mechanisms of the Atlantic meridional overturning circulation: a review. Rev Geophys. https://doi.org/10.1002/2015RG000493

Cheng W, Chiang JCH, Zhang D (2013) Atlantic meridional overturning circulation (AMOC) in CMIP5 Models: RCP and historical simulations. J Clim 26:7187–7197. https://doi.org/10.1175/JCLI-D-12-00496.1

Chiang JCH, Cheng W, Bitz CM (2008) Fast teleconnections to the tropical Atlantic sector from Atlantic thermohaline adjustment. Geophys Res Lett 35:L07704. https://doi.org/10.1029/2008GL033292

Cunningham SA, Kanzow T, Rayner D et al (2007) Temporal variability of the Atlantic meridional overturning circulation at 26.5°N. Science. https://doi.org/10.1126/science.1141304

Delworth TL, Greatbatch RJ (2000) Multidecadal thermohaline circulation variability driven by atmospheric surface flux forcing. J Clim. https://doi.org/10.1175/1520-0442(2000)013%3c1481:MTCVDB%3e2.0.CO;2

Delworth T, Manabe S, Stouffer RJ (1993) Interdecadal variations of the thermohaline circulation in a coupled ocean-atmosphere model. J Clim 6:1993–2011

Delworth TL, Broccoli AJ, Rosati A et al (2006) GFDL's CM2 Global coupled climate models. Part I: formulation and simulation characteristics. J Clim 19:643–674

Dickson RR, Meincke J, Malmberg SA, Lee AJ (1988) The "great salinity anomaly" in the Northern North Atlantic 1968–1982. Prog Oceanogr. https://doi.org/10.1016/0079-6611(88)90049-3

Donohoe A, Marshall J, Ferreira D, Mcgee D (2013) The relationship between ITCZ location and cross-equatorial atmospheric heat transport: from the seasonal cycle to the last glacial maximum. J Clim 26:3597–3618. https://doi.org/10.1175/JCLI-D-12-00467.1

Ek MB (2003) Implementation of Noah land surface model advances in the National Centers for Environmental Prediction operational mesoscale Eta model. J Geophys Res. https://doi.org/10.1029/2002JD003296

Endo H, Kitoh A (2014) Thermodynamic and dynamic effects on regional monsoon rainfall changes in a warmer climate. Geophys Res Lett 41:1704–1710. https://doi.org/10.1002/2013GL059158

Frierson DMW, Hwang Y-T, Fučkar NS et al (2013) Contribution of ocean overturning circulation to tropical rainfall peak in the Northern Hemisphere. Nat Geosci 6:940–944. https://doi.org/10.1038/ngeo1987

Ganai M, Phani Murali Krishna R, Mukhopadhyay P, Mahakur M (2015) The impact of revised simplified Arakawa-Schubert scheme on the simulation of mean and diurnal variability associated with active and break phases of of Indian summer monsoon using CFSv2. J Geophys Res Atmos. https://doi.org/10.1002/2014JD021636.Received

Gregory JM, Dixon KW, Stouffer RJ et al (2005) A model intercomparison of changes in the Atlantic thermohaline circulation in response to increasing atmospheric CO2 concentration. Geophys Res Lett. https://doi.org/10.1029/2005GL023209

Gregory JM, Bouttes N, Griffies SM et al (2016a) The Flux-Anomaly-Forced Model Intercomparison Project (FAFMIP) contribution to CMIP6: investigation of sea-level and ocean climate change in response to CO_2 forcing. Geosci Model Dev. https://doi.org/10.5194/gmd-9-3993-2016

Gregory JM, Bouttes N, Griffies SM et al (2016b) The flux-anomaly-forced model intercomparison project (FAFMIP) contribution to CMIP6: investigation of sea-level and ocean climate change in response to CO_2 forcing. Geosci Model Dev 9:3993–4017. https://doi.org/10.5194/gmd-9-3993-2016

Griffies SM (2009) Elements of MOM4p1, GFDL Ocean Group Technical Report 6. NOAA/Geophysical Fluid Dynamics Laboratory.

Griffies SM, Tziperman E (1995) A linear thermohaline oscillator driven by stochastic atmospheric forcing. J Clim. https://doi.org/10.1175/1520-0442(1995)008%3c2440:ALTODB%3e2.0.CO;2

Han J, Pan H-L (2011) Revision of convection and vertical diffusion schemes in the NCEP global forecast system. Weather Forecast 26:520–533. https://doi.org/10.1175/WAF-D-10-05038.1

Haug G, Hughen K (2000) Southward migration of the intertropical convergence zone through. Science 254:487–504. https://doi.org/10.1126/science.1059725

Haug GH, Hughen KA, Sigman DM et al (2001) Southward migration of the intertropical convergence zone through the holocene. Science. https://doi.org/10.1126/science.1059725

Haywood JM, Jones A, Dunstone N et al (2016) The impact of equilibrating hemispheric albedos on tropical performance in the HadGEM2-ES coupled climate model. Geophys Res Lett 43:395–403. https://doi.org/10.1002/2015GL066903

Hsu PC, Li T, Murakami H, Kitoh A (2013) Future change of the global monsoon revealed from 19 CMIP5 models. J Geophys Res Atmos. https://doi.org/10.1002/jgrd.50145

Huang P, Xie S, Hu K et al (2013) Patterns of the seasonal response of tropical rainfall to global warming. Nat Geosci 6:357–361. https://doi.org/10.1038/ngeo1792

Huffman GJ, Bolvin DT, Nelkin EJ et al (2007) The TRMM multisatellite precipitation analysis (TMPA): quasi-global, Multiyear, Combined-Sensor Precipitation Estimates at Fine Scales. J Hydrometeorol. https://doi.org/10.1175/JHM560.1

Jackson LC (2013) Shutdown and recovery of the AMOC in a coupled global climate model: the role of the advective feedback. Geophys Res Lett 40:1182–1188. https://doi.org/10.1002/grl.50289

Johns WE, Beal LM, Baringer MO et al (2008) Variability of shallow and deep western boundary currents off the Bahamas during 2004–05: results from the 26°N RAPID–MOC Array. J Phys Oceanogr 38:605–623. https://doi.org/10.1175/2007JPO3791.1

Johns WE, Baringer MO, Beal LM et al (2011) Continuous, array-based estimates of atlantic ocean heat transport at 26.5°N. J Clim. https://doi.org/10.1175/2010jcli3997.1

Kanzow T, Cunningham SA, Rayner D et al (2007) Observed flow compensation associated with the MOC at 26.5°N in the Atlantic. Science. https://doi.org/10.1126/science.1141293

Kanzow T, Cunningham SA, Johns WE et al (2010a) Seasonal variability of the Atlantic meridional overturning circulation at 26.5°N. J Clim. https://doi.org/10.1175/2010jcli3389.1

Kanzow T, Cunningham SA, Johns WE et al (2010b) Seasonal variability of the Atlantic meridional overturning circulation at 26.5°N. J Clim 23:5678–5698. https://doi.org/10.1175/2010JCLI3389.1

Kirtman B, Power SB, Adedoyin JA, et al (2013) Near-term Climate Change: Projections and Predictability. In: Climate Change 2013 the Physical Science Basis: Working Group I Contribution to the Fifth Assessment Report of the Intergovernmental Panel on Climate Change

Kitoh A, Yukimoto S, Noda A, Motoi T (1997) Simulated changes in the Asian summer monsoon at times of increased atmospheric CO_2. J Meteorol Soc Jpn Ser II 75:1019–1031. https://doi.org/10.2151/jmsj1965.75.6_1019

Kripalani RH, Oh JH, Kulkarni A et al (2007) South Asian summer monsoon precipitation variability: coupled climate model simulations and projections under IPCC AR4. Theor Appl Climatol 90:133–159. https://doi.org/10.1007/s00704-006-0282-0

Lau K-M, Li M-T (1984) The monsoon of East Asia and its global associations: a survey. Bull Am Meteorol Soc. https://doi.org/10.1175/1520-0477(1984)065%3c0114:tmoeaa%3e2.0.co;2

Lee JY, Wang B (2014) Future change of global monsoon in the CMIP5. Clim Dyn 42:101–119. https://doi.org/10.1007/s00382-012-1564-0

Li C, Yanai M (1996) The onset and interannual variability of the asian summer monsoon in relation to land-sea thermal contrast. J Clim. https://doi.org/10.1175/1520-0442(1996)009%3c0358:TOAIVO%3e2.0.CO;2

Li X, Ting M, Li C, Henderson N (2015) Mechanisms of Asian summer monsoon changes in response to anthropogenic forcing in CMIP5 models. J Clim 28:4107–4125. https://doi.org/10.1175/JCLI-D-14-00559.1

Liu W, Fedorov AV (2019) Global impacts of arctic sea ice loss mediated by the Atlantic meridional overturning circulation. Geophys Res Lett 46:944–952. https://doi.org/10.1029/2018GL080602

Locarnini RA, Mishonov AV, Antonov JI, Boyer TP, Garcia HE, Baranova OK, Zweng MM, Johnson DR (2010) World Ocean Atlas 2009, Volume 1: Temperature. In: Levitus S (ed) NOAA Atlas NESDIS 68. U.S. Government Printing Office, Washington, DC, p 184

Mantsis DF, Clement AC (2009) Simulated variability in the mean atmospheric meridional circulation over the 20th century. Geophys Res Lett. https://doi.org/10.1029/2008GL036741

McCarthy G, Frajka-Williams E, Johns WE et al (2012) Observed interannual variability of the Atlantic meridional overturning circulation at 26.5°N. Geophys Res Lett. https://doi.org/10.1029/2012gl052933

McGee D, Donohoe A, Marshall J, Ferreira D (2014) Changes in ITCZ location and cross-equatorial heat transport at the last glacial maximum, Heinrich Stadial 1, and the mid-Holocene. Earth Planet Sci Lett. https://doi.org/10.1016/j.epsl.2013.12.043

McGee D, Moreno-Chamarro E, Green B et al (2018) Hemispherically asymmetric trade wind changes as signatures of past ITCZ shifts. Q Sci Rev 180:214–228. https://doi.org/10.1016/j.quascirev.2017.11.020

Meehl GA, Arblaster JM, Tebaldi C (2005) Understanding future patterns of increased precipitation intensity in climate model simulations. Geophys Res Lett. https://doi.org/10.1029/2005GL023680

Mei R, Ashfaq M, Rastogi D et al (2015) Dominating controls for wetter South Asian summer monsoon in the twenty-first century. J Clim 28:3400–3419. https://doi.org/10.1175/JCLI-D-14-00355.1

Menon A, Levermann A, Schewe J et al (2013) Consistent increase in Indian monsoon rainfall and its variability across CMIP-5 models. Earth Syst Dyn 4:287–300. https://doi.org/10.5194/esd-4-287-2013

Mikolajewicz U, Voss R (2000) The role of the individual air-sea flux components in CO_2-induced changes of the ocean's circulation and climate. Clim Dyn. https://doi.org/10.1007/s003820000066

Mohtadi M, Prange M, Oppo DW et al (2014) North Atlantic forcing of tropical Indian Ocean climate. Nature 509:76

Moorthi S, Pan HL, Caplan P (2001) Changes to the 2001 NCEP operational MRF/AVN global analysis/forecast system. NWS Technical Procedures Bulletin 484. NCEP, Silver Spring, MD, p 14

Parsons LA, Yin J, Overpeck JT et al (2014) Influence of the Atlantic meridional overturning circulation on the monsoon rainfall and carbon balance of the American tropics. Geophys Res Lett 41:146–151. https://doi.org/10.1002/2013GL058454

Rahmstorf S, Ganopolski A (1999) Long-term global warming scenarios computed with an efficient coupled climate model. Clim Change. https://doi.org/10.1023/A:1005474526406

Rahmstorf S, Box JE, Feulner G et al (2015) Exceptional twentieth-century slowdown in Atlantic Ocean overturning circulation. Nat Clim Change 5:475–480. https://doi.org/10.1038/nclimate2554

Rajeevan M, Gadgil S, Bhate J (2010) Active and break spells of the indian summer monsoon. J Earth Syst Sci. https://doi.org/10.1007/s12040-010-0019-4

Rayner NA, Parker DE, Horton EB et al (2003) Global analyses of sea surface temperature, sea ice, and night marine air temperature since the late nineteenth century. J Geophys Res 108:4407. https://doi.org/10.1029/2002JD002670

Rayner D, Hirschi JJM, Kanzow T et al (2011) Monitoring the Atlantic meridional overturning circulation. Deep Res Part II Top Stud Oceanogr. https://doi.org/10.1016/j.dsr2.2010.10.056

Rhein M (2014) Observations: ocean pages. Clim Change 2013. Phys Sci Basis. https://doi.org/10.1017/cbo9781107415324.010

Saha A, Ghosh S, Sahana AS, Rao EP (2014) Failure of CMIP5 climate models in simulating post-1950 decreasing trend of Indian monsoon. Geophys Res Lett 41:7323–7330. https://doi.org/10.1002/2014GL061573

Sévellec F, Fedorov AV, Liu W (2017) Arctic sea-ice decline weakens the Atlantic meridional overturning circulation. Nat Clim Chang 7:604–610. https://doi.org/10.1038/NCLIMATE3353

Sikka DR, Gadgil S (1980) On the Maximum Cloud Zone and the ITCZ over Indian, Longitudes during the Southwest Monsoon. Mon Weather Rev 108:1840–1853

Sinha A, Kathayat G, Cheng H et al (2015) Trends and oscillations in the Indian summer monsoon rainfall over the last two millennia. Nat Commun 6:1–8. https://doi.org/10.1038/ncomms7309

Srokosz M, Baringer M, Bryden H et al (2012) Past, present, and future changes in the atlantic meridional overturning circulation. Bull Am Meteorol Soc. https://doi.org/10.1175/BAMS-D-11-00151.1

Stocker TF, Allen SK, Bex V, Midgley PM (2013) Climate change 2013 The Physical Science Basis Working Group I Contribution to the Fifth Assessment Report of the Intergovernmental Panel on Climate Change

Stouffer RJ, Yin J, Gregory JM et al (2006) Investigating the cause of the response of the thermohaline circulation to past and future climage changes. J Clim. https://doi.org/10.1175/JCLI3689.1

Stowasser M, Annamalai H, Hafner J (2009) Response of the South Asian summer monsoon to global warming: mean and synoptic systems. J Clim 22:1014–1036. https://doi.org/10.1175/2008JCLI2218.1

Sun Y, Clemens SC, Morrill C et al (2011) Influence of Atlantic meridional overturning circulation on the East Asian winter monsoon. Nat Geosci 5:46–49. https://doi.org/10.1038/ngeo1326

Sun C, Li J, Jin FF, Ding R (2013) Sea surface temperature inter-hemispheric dipole and its relation to tropical precipitation. Environ Res Lett. https://doi.org/10.1088/1748-9326/8/4/044006

Sutton RT, Hodson DLR (2005) Ocean science: Atlantic ocean forcing of North American and European summer climate. Science. https://doi.org/10.1126/science.1109496

Swapna P, Roxy MK, Aparna K et al (2014) The IITM earth system model: transformation of a seasonal prediction model to a long term climate model. Bull Am Meteorol Soc 96:115–119

Swapna P, Krishnan R, Sandeep N et al (2018) Long-Term climate simulations using the IITM earth system model (IITM-ESMv2) with focus on the south asian monsoon. J Adv Model Earth Syst 10:1127–1149. https://doi.org/10.1029/2017MS001262

Tanaka HL, Ishizaki N, Nohara D (2005) Intercomparison of the intensities and trends of hadley, walker and monsoon circulations in the global warming projections. SOLA. https://doi.org/10.2151/sola.2005-021

Taylor KE, Stouffer RJ, Meehl GA (2012) An overview of CMIP5 and the experiment design. Bull Am Meteorol Soc 93:485–498. https://doi.org/10.1175/BAMS-D-11-00094.1

Trenberth KE (1998) Atmospheric moisture residence times and cycling: implications for rainfall rates and climate change. Clim Change. https://doi.org/10.1023/A:1005319109110

Trenberth KE, Fasullo JT (2017) Atlantic meridional heat transports computed from balancing Earth's energy locally. Geophys Res Lett. https://doi.org/10.1002/2016GL072475

Turner AG, Annamalai H (2012) Climate change and the South Asian summer monsoon. Nat Clim Change 2:587–595. https://doi.org/10.1038/nclimate1495

Ueda H, Iwai A, Kuwako K, Hori ME (2006) Impact of anthropogenic forcing on the Asian summer monsoon as simulated by eight GCMs. Geophys Res Lett. https://doi.org/10.1029/2005GL025336

Vellinga M, Wood RA (2002) Global climatic impacts of a collapse of the Atlantic thermohaline circulation. Clim Change. https://doi.org/10.1023/A:1016168827653

Vellinga M, Wood RA (2008) Impacts of thermohaline circulation shutdown in the twenty-first century. Clim Change 91:43–63. https://doi.org/10.1007/s10584-006-9146-y

Vial J, Cassou C, Codron F et al (2018) Influence of the Atlantic meridional overturning circulation on the tropical climate response to CO_2 forcing. Geophys Res Lett. https://doi.org/10.1029/2018GL078558

Voigt A, Stevens B, Bader J, Mauritsen T (2013) The observed hemispheric symmetry in reflected shortwave irradiance. J Clim 26:468–477. https://doi.org/10.1175/JCLI-D-12-00132.1

Wang YJ, Cheng H, Edwards RL et al (2001) A high-resolution absolute-dated late pleistocene monsoon record from Hulu cave, China. Science. https://doi.org/10.1126/science.1064618

Wang J, Yang B, Ljungqvist FC et al (2017) Internal and external forcing of multidecadal Atlantic climate variability over the past 1,200 years. Nat Geosci. https://doi.org/10.1038/ngeo2962

Webster PJ, Magaña VO, Palmer TN et al (1998) Monsoons: processes, predictability, and the prospects for prediction. J Geophys Res 103:14451. https://doi.org/10.1029/97JC02719

Winton M (2000) A reformulated three-layer sea ice model. J Atmos Ocean Technol 17:525–531. https://doi.org/10.1175/1520-0426(2000)017%3c0525:ARTLSI%3e2.0.CO;2

Woollings T, Gregory JM, Pinto JG et al (2012) Response of the North Atlantic storm track to climate change shaped by ocean atmosphere coupling. Nat Geosci 5:313–317. https://doi.org/10.1038/ngeo1438

Xavier PK, Marzin C, Goswami BN (2007) An objective definition of the Indian summer monsoon season and a new perspective on the ENSO–monsoon relationship. Q J R Metero Soc A 133:937–948.

Zhang R, Delworth TL (2005) Simulated tropical response to a substantial weakening of the Atlantic thermohaline circulation. J Clim 18:1853–1860. https://doi.org/10.1175/JCLI3460.1

Zhang R, Delworth TL (2006) Impact of Atlantic multidecadal oscillations on India/Sahel rainfall and Atlantic hurricanes. Geophys Res LEtt 33:1–5. https://doi.org/10.1029/2006GL026267